Contents lists available at ScienceDirect

Arabian Journal of Chemistry

journal homepage: www.ksu.edu.sa

Contamination and health risk assessment of potentially toxic elements in agricultural soil of the Al-Ahsa Oasis, Saudi Arabia using health indices and GIS

Talal Alharbi, Abdelbaset S. El-Sorogy *, Khaled Al-Kahtany

Geology and Geophysics Department, College of Science, King Saud University, Saudi Arabia

ARTICLE INFO

Keywords:
Hazard index
Chronic daily intake
Lead
Arsenic
Chromium
Saudi Arabia

ABSTRACT

The current work aimed to assess contamination and human health risk of potentially toxic elements (PTEs) in agricultural soil of the Al-Ahsa Oasis, Saudi Arabia. For the purpose of evaluating the potential risks to human health associated with ingestion, skin contact, and inhalation, the chronic daily intake (CDI), hazard quotient (HQ), hazard index (HI), cancer risk (CR), and total lifetime cancer risk (LCR) were calculated in 30 soil samples. The spatial distribution and possible sources of HMs were investigated using GIS and multivariate analysis. The descending order of PTE averages (dw, μg/g) was Fe (11790) > Mn (176.43) > Zn (54.43) > Cr (28.67) > Ni (14.53) > V (12.33) > Cu (10.83) > Pb (5.23) > Co (2.87) > As (2.27). The average CDI for all PTEs from ingestion pathway in children indicates an increase of approximated 9 times compared to adults. The HI values varied from 1.969×10^{-4} to 2.318×10^{-2} for Adults, and from 1.835×10^{-3} to 2.158×10^{-1} for children, suggesting there is no significant non-carcinogenic risk to the people inhabiting the Al-Ahsa Oasis. The CRs and LCR for Cr, As, and Pb in children was found to be significantly greater than that of adults. LCR values for As, Pb, and Cr varied from lower than 1×10^{-6} to 1×10^{-4}, indicating no significant health hazards to acceptable carcinogenic risk.

1. Introduction

In the last decade, enormous increase in industrialization, rapid urbanization and population growth have resulted in the production of huge quantities of solid and liquid waste including emission of potentially toxic elements (PTEs) in various ecological compartments that drastically deteriorated water quality and threatened aquatic life and human health (El-Sorogy et al., 2016, 2021, 2023; Al-Hashim et al., 2022; Kahal et al., 2023). Agricultural soil is essential for food safety and has a direct impact on human health (Praveena et al., 2015; Agyeman et al., 2021, Alarifi et al., 2023). Unfortunately, dumping of domestic and industrial effluents ultimately contaminate soil with huge quantities of PTEs and become a hazard for the animals and human being (Hashem et al., 2017; Mishra et al., 2019).

Generally, both natural and anthropogenic factors add PTEs to soils and crops. Above-normal concentrations of PTEs can be found in agricultural soils as a result of rock weathering, and volcanic activity. The primary human sources include land amendments made from sewage sludge, livestock manure, wastewater irrigation, metal-based insecticides and herbicides, and fertilizers based on phosphate (El-Kady and Abdel-Wahhab, 2018). Agriculture is severely affected mainly due to usage of industrial wastewater for irrigation resulting in increased contamination of Cd, Pb, Cr, As and other metals in crops (Ilyas et al., 2019).

PTEs are the most hazardous contaminants for human being causing severe complications due to their build-up in crops (Zhang et al., 2018). Children are more vulnerable to HMs due to additional pathways of exposure such as placental exposure, nursing, early-life hand-to-mouth activities, and larger comparative uptakes (Dissanayake and Chandrajith, 2009; Rahman et al., 2021). Of all the metal pollutants major threats to human health emanate from exposure to non-essential PTEs such as As, Cd, Pb and Hg. These metals can enter the human body primarily through ingestion, inhalation, and skin adsorption and can be found in a variety of environmental compartments, including food, water, and air. Consuming tainted food items, including fruits, vegetables, shellfish, fish, and drinking water and beverages, is the primary

Peer review under responsibility of King Saud University.
* Corresponding author. P.O Box: 2455, Riyadh 11451, Saudi Arabia.
E-mail address: asmohamed@ksu.edu.sa (A.S. El-Sorogy).

https://doi.org/10.1016/j.arabjc.2023.105592
Received 6 November 2023; Accepted 25 December 2023
Available online 30 December 2023

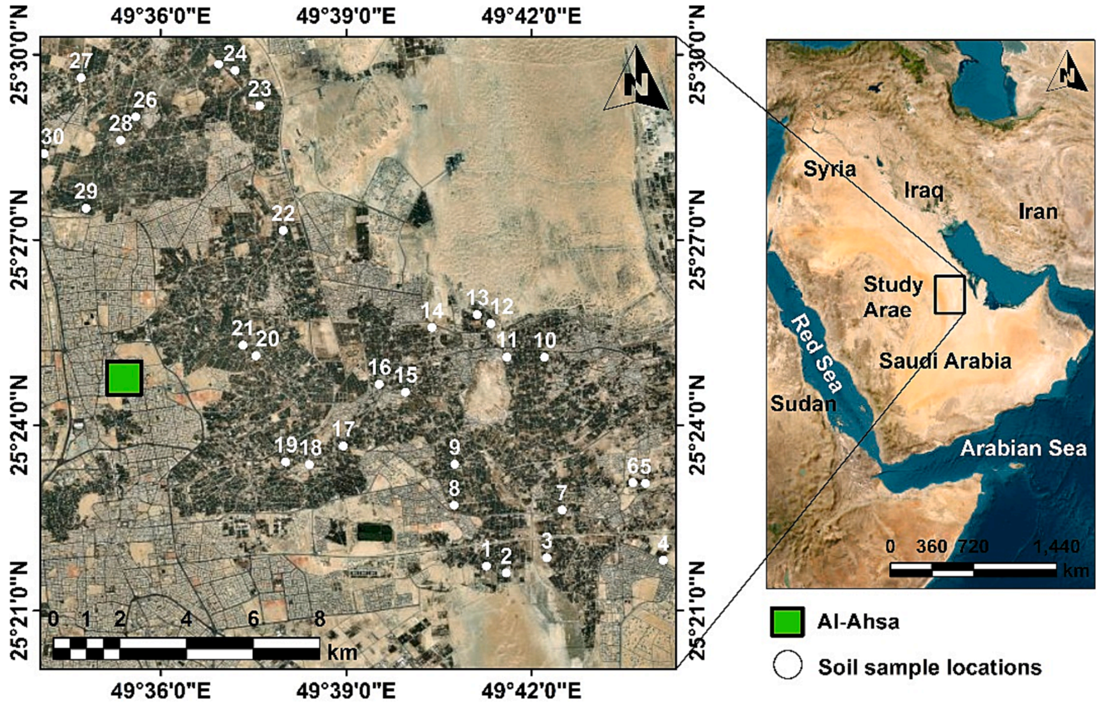

Fig. 1. Location map of the sampling sites at Al-Ahsa Oasis.

Table 1
Elemental analysis by ICP–AES (dw, μg/g) of sampling sites at Al-Ahsa Oasis.

S.N.	As	Co	Cr	Cu	Fe	Mn	Ni	Pb	V	Zn
S1	4.00	3.00	23	9.00	11,200	188	18.00	5.00	16.00	42.00
S2	3.00	3.00	25	9.00	13,800	194	20.00	5.00	17.00	46.00
S3	2.00	3.00	45	17.00	12,300	219	16.00	5.00	13.00	62.00
S4	2.00	3.00	20	12.00	10,800	164	13.00	3.00	11.00	53.00
S5	1.00	3.00	28	15.00	13,500	216	20.00	6.00	16.00	54.00
S6	4.00	6.00	54	17.00	19,800	327	38.00	11.00	31.00	100.00
S7	3.00	4.00	50	10.00	11,600	178	19.00	11.00	15.00	30.00
S8	2.00	4.00	26	9.00	12,000	162	18.00	8.00	15.00	33.00
S9	2.00	3.00	26	7.00	11,600	159	14.00	4.00	11.00	16.00
S10	4.00	4.00	59	10.00	10,300	166	21.00	6.00	15.00	28.00
S11	2.00	2.00	17	5.00	8400	115	8.00	5.00	7.00	17.00
S12	1.00	3.00	22	18.00	14,600	222	11.00	3.00	10.00	55.00
S13	2.00	3.00	26	17.00	11,300	192	13.00	4.00	10.00	68.00
S14	2.00	3.00	43	7.00	9500	134	17.00	6.00	18.00	12.00
S15	1.00	2.00	63	18.00	11,100	152	17.00	7.00	15.00	447.00
S16	1.00	1.00	12	6.00	7000	100	8.00	4.00	8.00	21.00
S17	2.00	3.00	24	10.00	10,200	147	16.00	6.00	13.00	31.00
S18	2.00	3.00	22	9.00	14,200	194	16.00	4.00	11.00	43.00
S19	2.00	4.00	77	14.00	11,600	198	24.00	10.00	19.00	45.00
S20	2.00	2.00	13	10.00	11,300	141	6.00	3.00	7.00	19.00
S21	3.00	4.00	26	10.00	12,800	196	18.00	7.00	16.00	21.00
S22	2.00	2.00	15	9.00	11,700	187	10.00	5.00	8.00	44.00
S23	2.00	1.00	11	4.00	10,500	131	5.00	2.00	5.00	19.00
S24	1.00	2.00	16	6.00	9000	139	9.00	3.00	10.00	45.00
S25	4.00	3.00	18	8.00	13,800	173	14.00	4.00	12.00	23.00
S26	5.00	3.00	23	14.00	11,300	186	10.00	5.00	9.00	58.00
S27	2.00	2.00	21	7.00	9600	139	10.00	4.00	9.00	16.00
S28	2.00	2.00	24	6.00	10,100	140	9.00	3.00	7.00	25.00
S29	1.00	3.00	15	25.00	15,600	274	8.00	4.00	7.00	126.00
S30	2.00	2.00	16	7.00	13,200	160	10.00	4.00	9.00	34.00
Min.	1.00	1.00	11	4.00	7000	100.00	5.00	2.00	5.00	12.00
Max.	5.00	6.00	77	25.00	19,800	327.00	38.00	11.00	31.00	447.00
Std. Dev.	1.05	1.01	16.77	4.89	2427	45.89	6.62	2.30	5.18	78.28

method by which humans are exposed to metals. The effects of metal poisoning on the human body are well-established and have been linked to numerous diseases, including mental illness, harm to the kidneys, liver, lungs, and other essential organs, as well as changes to the components of blood (Jaishankar et al., 2014; Alharbi et al., 2023a, b; Al-Kahtany et al., 2023a).

Al-Ahsa is the largest oasis in Saudi Arabia's Eastern Province, covering ~ 12,000 ha. The soil composition in Saudi Arabia displays a diversity of types determined by their mineralogical properties and the underlying rocks. In the eastern region, the soils vary from Torrifluvents

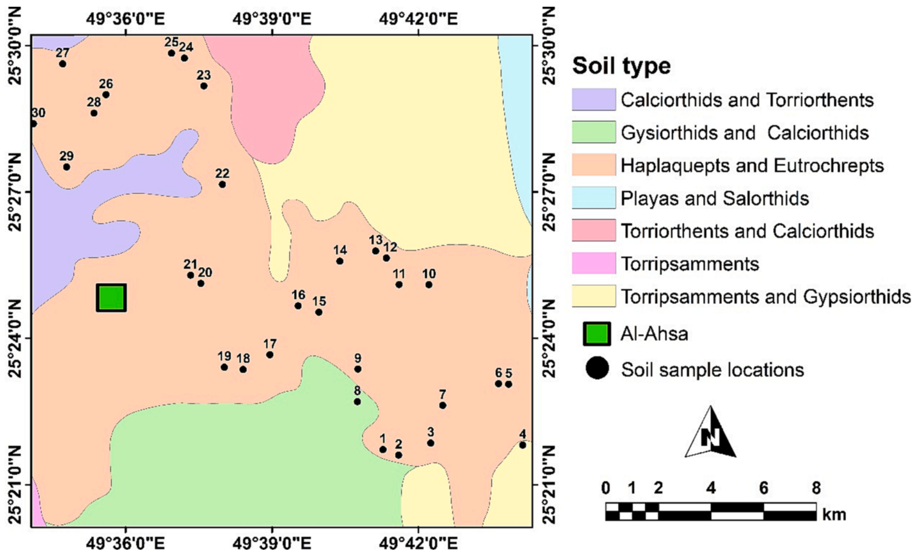

Fig. 2. Soil types in Al Ahsa Oasis.

Table 2
The average values of PTEs (μg/g) in the study area and the comparison with those reported in the earth's crust and international backgrounds.

Location and reference	Ni	Zn	Cu	As	Pb	Cr	V	Co	Fe	Mn
Study area	14.53	54.43	10.83	2.27	5.23	28.67	12.33	2.87	11,790	176.43
Al-Ammariah, Saudi Arabia (Alarifi et al., 2022)	26.94	52.16	11.36	3.78	5.08	19.97	18.94	3.89	11,581	179.61
Al Uyaynah–Al Jubailah soil, Saudi Arabia (Alharbi and El-Sorogy, 2021)	19.25	64.33	10.56	13.8	28.48	30.18	ND	2.45	35,667	ND
Wadi Jazan, Saudi Arabia (Al-Boghdady and Hassanein, 2019)	48.66	75.80	72.85	14.13	19.41	77.22	122.03	7722	23,811	583.58
Worldwide soils (Kabata-Pendias (2011)	29	70	38.9	6.83	27	59.5	129	11.3	35,000	488
Earth's crust (Yaroshevsky, 2006)	58	83	47	1.7	16	83	90	18	46,500	1000
Continental crust (Rudnick and Gao, 2003)	47	67	28	4.8	17	92	97	17.3	50,400	1000
Earth's crust (Turekian and Wedepohl, 1961)	68	95	45	13	20	90	130	19	47,200	850
Continental crust (Taylor, 1964)	75	70	55	1.8	12.5	100	135	25	56,300	950
Maximum allowable concentrations Kabata-Pendias (2011)	60	300	150	20	300	200	150	50	ND	ND

to Gypsiorthids, characterized by coarse texture and elevated levels of salt, gypsum, and carbonate contents (Shadfan et al., 1987). The farming of primarily dates, leafy green plants, vegetables, and fruits is performed in this region (Al Tokhais and Rausch, 2008). Al-Ahsa's groundwater levels have steadily declined over time as a result of overusing water resources to irrigate large areas of farmland. Therefore, part of the sewage water produced by the Saudi Aramco plant, the Hofuf, Al-Ayoun, and Al-Omran sewage treatment facilities, is used to meet the water needs of industry and agriculture. These plants treat residential and industrial sewage as well as agricultural drainage water. To avoid health risks, sewage water must be effectively treated before its reuse in agricultural practices (Chowdhury and Al-Zahrani, 2015). The objectives of this study are threefold: (i) to document the characteristics of Al Ahsa soils and their Ni, Fe, Mn, Zn, Cu, As, Pb, Cr, V, and Co contents; (ii) to compare the PTEs levels in the study area with those reported from local and regional soils and backgrounds; and (iii) to assess the human health risk of PTEs associated with ingestion, skin contact, and inhalation **in the study area.**

2. Materials and methods

2.1. Study area

Al-Ahsa is situated 320 km away from Riyadh and 75 km away from the Arabian Gulf shore. The study region is located between N25°21′00–N25°37′00 and E49°33′00–E49°46′00 (Fig. 1). Al-Ahsa is an arid region with long and scorching summers that exhibits a wide range of annual fluctuations in temperature, humidity, evaporation, and precipitation. The average temperature and evaporation rates are extremely high at 43 °C and 12 mm, respectively, and humidity decreases to a minimum of 20 %. On the other hand, winters are quite chilly, with daytime highs of 20–28 °C and evening lows of 8–10 °C. The average annual precipitation is 147 mm, the average humidity is 71 %, and the average evaporation rate is 5 mm.

Al-Ahsa is located on a sedimentary succession comprising carbonates, evaporates, and subordinate marl and shale, with a total thickness of 800–2,500 m, which increases and slopes toward the Arabian Gulf. The sedimentary strata are interrupted by several north–south anticlines and synclines, which are the main tectonic elements in Saudi Arabia's Eastern Province. Four partially interconnected aquifers compose the groundwater system in this area (Assubaie, 2015): from top to bottom, i) karstified fractured bedrock and unconsolidated porous classics of the Neogene aquifer complex with a depth of up to 180 m, ii) partly karstified fractured bedrocks of the Dammam aquifer complex with depths of 180–250 m, and iii) and iv) karstified fractured bedrocks of the Umm Er Radhuma and Aruma aquifers with depth of 240–280 m.

2.2. Sampling and analytical procedures

From palm farms in the Al-Ahsa Oasis, thirty soil samples were taken (Fig. 1). Samples were collected using a plastic hand trowel at a depth of less than 5 cm from the soil's surface (3 replicates from each site). Subsequently, the samples were placed in plastic sample bags and stored in an icebox. The collected samples underwent sieving and were then left to air dry. A prepared sample (0.50 g) with a fraction of < 63 μm was incubated with a HNO_3–HCl aqua regia for 45 min in a graphite heating block. After cooling, the resultant solution was diluted to 12.5 mL using deionized water, mixed, and analyzed. Ni, Fe, Mn, Zn, Cu, As, Pb, Cr, V,

Table 3
The CDI (mg/kg/day), HQ, and HI for non-carcinogenic risk in adults and children.

HMs	Adults						
	CDI Ing.	**CDI Dermal**	**CDI Inhal.**	**HQ Ing.**	**HQ Demal**	**HQ Inhal.**	**HI**
As	3.105 × 10–6	1.093 × 10–8	4.566 × 10–11	1.035 × 10–2	3.644 × 10–5	1.522 × 10–7	1.039 × 10–2
Cr	3.927 × 10–5	8.745 × 10–8	5.775 × 10–10	1.309 × 10–2	2.915 × 10–5	1.925 × 10–7	1.312 × 10–2
Pb	7.169 × 10–6	2.186 × 10–8	1.054 × 10–10	2.048 × 10–3	6.247 × 10–6	3.012 × 10–8	2.055 × 10–2
V	1.690 × 10–5	4.919 × 10–8	2.485 × 10–10	1.877 × 10–3	5.466 × 10–6	2.761 × 10–8	1.883 × 10–3
Cu	1.484 × 10–5	3.826 × 10–8	2.182 × 10–10	4.000 × 10–4	1.031 × 10–6	5.882 × 10–9	4.010 × 10–4
Ni	1.991 × 10–5	5.466 × 10–8	2.928 × 10–10	9.703 × 10–4	2.733 × 10–6	1.427 × 10–8	9.731 × 10–4
Zn	7.457 × 10–5	1.858 × 10–7	1.097 × 10–9	2.486 × 10–4	6.195 × 10–7	3.655 × 10–9	2.492 × 10–4
Co	3.927 × 10–6	1.093 × 10–8	5.775 × 10–11	1.963 × 10–4	5.466 × 10–7	2.888 × 10–9	1.969 × 10–4
Fe	1.615 × 10–2	7.215 × 10–5	2.375 × 10–7	2.307 × 10–2	1.031 × 10–4	3.393 × 10–7	2.318 × 10–2
Mn	2.417 × 10–4	8.745 × 10–7	3.554 × 10–9	1.726 × 10–3	6.247 × 10–6	2.539 × 10–8	1.733 × 10–3
HMs	Children						
	CDI Ing.	CDI Dermal	CDI Inhal.	HQ Ing.	HQ Demal	HQ Inhal.	Hi
As	2.898 × 10–5	5.101 × 10–8	2.131 × 10–10	9.660 × 10–2	1.700 × 10–4	7.103 × 10–7	9.677 × 10–2
Cr	3.665 × 10–4	4.081 × 10–7	2.695 × 10–9	1.222 × 10–1	1.360 × 10–4	8.983 × 10–7	1.223 × 10–2
Pb	6.691 × 10–5	1.020 × 10–7	4.912 × 10–10	1.912 × 10–2	2.915 × 10–5	1.406 × 10–7	1.915 × 10–2
V	1.577 × 10–4	2.296 × 10–7	1.159 × 10–9	1.752 × 10–2	2.551 × 10–5	1.288 × 10–7	1.755 × 10–2
Cu	1.385 × 10–4	1.785 × 10–7	1.018 × 10–9	3.733 × 10–3	4.813 × 10–6	2.745 × 10–8	3.738 × 10–3
Ni	1.858 × 10–4	2.551 × 10–7	1.366 × 10–9	9.291 × 10–3	1.275 × 10–5	6.831 × 10–8	9.304 × 10–3
Zn	6.960 × 10–4	8.672 × 10–7	5.117 × 10–9	2.320 × 10–3	2.891 × 10–6	1.706 × 10–8	2.323 × 10–3
Co	3.665 × 10–5	5.101 × 10–8	2.695 × 10–10	1.833 × 10–3	2.551 × 10–6	1.347 × 10–8	1.835 × 10–3
Fe	1.507 × 10–1	3.367 × 10–4	1.108 × 10–6	2.153 × 10–1	4.890 × 10–4	1.583 × 10–6	2.158 × 10–1
Mn	2.256 × 10–3	4.081 × 10–6	1.659 × 10–8	1.611 × 10–2	2.915 × 10–5	1.185 × 10–7	1.614 × 10–2

and Co were analyzed in terms of linearity, limit of detection, limit of quantification, accuracy, and precision using inductively coupled plasma-atomic emission spectrometry (ICP–AES) in the ALS Geochemistry Lab, Jeddah, Saudi Arabia. Plotting the peak size of the ideal emission line as a function of a standard or spike solution concentration for standard addition curves allowed graphs representing the calibration curves of each element to be created. Excellent linearity was displayed by each calibration curve.

2.3. Data analysis

The Environmental Protection Agency of the United States assessed the health hazards associated with ingestion, inhalation, and skin contact pathways for both adults and children (US EPA, 2002). To define the CDI for the three pathways (mg/kg. day) the following equations were utilized: (Luo et al., 2012; Mondal et al., 2021; Agyeman et al., 2021; Ahmad et al., 2021):

$$CDI_{ingest.} = (Csoil \times IngR \times EF \times ED)/(BW \times AT) \times CF$$

$$CDI_{inhal.} = (Csoil. \times InhR \times EF \times ED)/(PEF \times BW \times AT)$$

$$CDI_{dermal} = (Csoil. \times SA \times AF \times ABF \times EF \times ED)/(BW \times AT) \times CF$$

C represents the concentration of PTEs in mg/kg. IngR denotes the ingestion rate in mg/day, with a value of 200 for children and 100 for adults. EF represents exposure frequency in days/year (180), while ED is the exposure duration (6 years for children and 24 years for adults). BW stands for the average body weight, set at 15 kg for children and 70 kg for adults. AT corresponds to the average time (365 × ED). InhR signifies the inhalation rate in mg/cm^2 (20 for both adults and children), and PEF is the particle emission factor in m^3 kg (1.36 × 109 for both adults and children). SA denotes the surface area of exposed skin in cm^2 (2145 for adults and 1150 for children), AF is the skin adherence factor for the soil in mg cm^2 (0.2 for adults and 0.07 for children), and ABF represents the dermal absorption factor (0.03 for As and 0.001 for other metals).

Cr, Pb and As were selected to estimate the carcinogenic health risks (IARC, 2012), whilst, V, Fe, As, Co, Ni, Zn, Cr, Pb, and Cu were also estimated for their non-carcinogenic risk. The hazard index (HI) is estimated by summing up all the hazard quotients (HQs), and gives the total risk of being non-carcinogenic for a single element as follows (Chonokhuu et al., 2019):

$$HI = \Sigma HQE = HQ_{ing} + HQ_{dermal} + HQ_{inhal}$$

$$HQE = CDI/RfD$$

where RfD is the reference dose for each PTE (Table 1). HI values less than one indicate no significant risk of non-carcinogenic effects, and HI values exceeds one indicate there is a probability that non-carcinogenic risk effects may occur, and the probability increases with increasing HI (USEPA, 2001; IRIS, 2020). The total lifetime cancer risk (LCR) was determined using the following equations:

$$Cancerrisk = CDI \times CSF$$

$$LCR = \Sigma CancerRisk = Cancerrisk_{ing} + Cancerrisk_{dermal} + Cancerrisk_{inhal}$$

where CSF is the carcinogenic slope factor values (mg/kg/day) for Cr, Pb and As (0.5, 0.0085 and 1.5, respectively) (IRIS, 2020). LCR values lower than 1 × 10^{-6} indicate no significant health hazards, LCR value between 1 × 10^{-6} and 1 × 10^{-4} indicates acceptable carcinogenic risk, and LCR value higher than 1 × 10^{-4} means the risk is unacceptable (USEPA, 1989; Mondal et al., 2021).

3. Results and discussion

3.1. Soil characteristics and distribution of PTEs

The process of land classification and survey in Saudi Arabia commenced in 1986, as documented by MEWA (1986) and Al-Dosary (2022). In the Al Ahsa Oasis, the soil can be categorized into Haplaquepts and Eutrochrepts (28 samples), Torripsamments and Gysiorthids

HMs	Adults						
	$CDI_{Ing.}$	CDI_{Dermal}	$CDI_{Inhal.}$	$HQ_{Ing.}$	HQ_{Demal}	$HQ_{Inhal.}$	HI
As	3.105×10^{-6}	1.093×10^{-8}	4.566×10^{-11}	1.035×10^{-2}	3.644×10^{-5}	1.522×10^{-7}	1.039×10^{-2}
Cr	3.927×10^{-5}	8.745×10^{-8}	5.775×10^{-10}	1.309×10^{-2}	2.915×10^{-5}	1.925×10^{-7}	1.312×10^{-2}
Pb	7.169×10^{-6}	2.186×10^{-8}	1.054×10^{-10}	2.048×10^{-3}	6.247×10^{-6}	3.012×10^{-8}	2.055×10^{-2}
V	1.690×10^{-5}	4.919×10^{-8}	2.485×10^{-10}	1.877×10^{-3}	5.466×10^{-6}	2.761×10^{-8}	1.883×10^{-3}
Cu	1.484×10^{-5}	3.826×10^{-8}	2.182×10^{-10}	4.000×10^{-4}	1.031×10^{-6}	5.882×10^{-9}	4.010×10^{-4}
Ni	1.991×10^{-5}	5.466×10^{-8}	2.928×10^{-10}	9.703×10^{-4}	2.733×10^{-6}	1.427×10^{-8}	9.731×10^{-4}
Zn	7.457×10^{-5}	1.858×10^{-7}	1.097×10^{-9}	2.486×10^{-4}	6.195×10^{-7}	3.655×10^{-9}	2.492×10^{-4}
Co	3.927×10^{-6}	1.093×10^{-8}	5.775×10^{-11}	1.963×10^{-4}	5.466×10^{-7}	2.888×10^{-9}	1.969×10^{-4}
Fe	1.615×10^{-2}	7.215×10^{-5}	2.375×10^{-7}	2.307×10^{-2}	1.031×10^{-4}	3.393×10^{-7}	2.318×10^{-2}
Mn	2.417×10^{-4}	8.745×10^{-7}	3.554×10^{-9}	1.726×10^{-3}	6.247×10^{-6}	2.539×10^{-8}	1.733×10^{-3}
HMs	Children						
	$CDI_{Ing.}$	CDI_{Dermal}	$CDI_{Inhal.}$	$HQ_{Ing.}$	HQ_{Demal}	$HQ_{Inhal.}$	Hi
As	2.898×10^{-5}	5.101×10^{-8}	2.131×10^{-10}	9.660×10^{-2}	1.700×10^{-4}	7.103×10^{-7}	9.677×10^{-2}
Cr	3.665×10^{-4}	4.081×10^{-7}	2.695×10^{-9}	1.222×10^{-1}	1.360×10^{-4}	8.983×10^{-7}	1.223×10^{-2}
Pb	6.691×10^{-5}	1.020×10^{-7}	4.912×10^{-10}	1.912×10^{-2}	2.915×10^{-5}	1.406×10^{-7}	1.915×10^{-2}
V	1.577×10^{-4}	2.296×10^{-7}	1.159×10^{-9}	1.752×10^{-2}	2.551×10^{-5}	1.288×10^{-7}	1.755×10^{-2}
Cu	1.385×10^{-4}	1.785×10^{-7}	1.018×10^{-9}	3.733×10^{-3}	4.813×10^{-6}	2.745×10^{-8}	3.738×10^{-3}
Ni	1.858×10^{-4}	2.551×10^{-7}	1.366×10^{-9}	9.291×10^{-3}	1.275×10^{-5}	6.831×10^{-8}	9.304×10^{-3}
Zn	6.960×10^{-4}	8.672×10^{-7}	5.117×10^{-9}	2.320×10^{-3}	2.891×10^{-6}	1.706×10^{-8}	2.323×10^{-3}
Co	3.665×10^{-5}	5.101×10^{-8}	2.695×10^{-10}	1.833×10^{-3}	2.551×10^{-6}	1.347×10^{-8}	1.835×10^{-3}
Fe	1.507×10^{-1}	3.367×10^{-4}	1.108×10^{-6}	2.153×10^{-1}	4.890×10^{-4}	1.583×10^{-6}	2.158×10^{-1}
Mn	2.256×10^{-3}	4.081×10^{-6}	1.659×10^{-8}	1.611×10^{-2}	2.915×10^{-5}	1.185×10^{-7}	1.614×10^{-2}

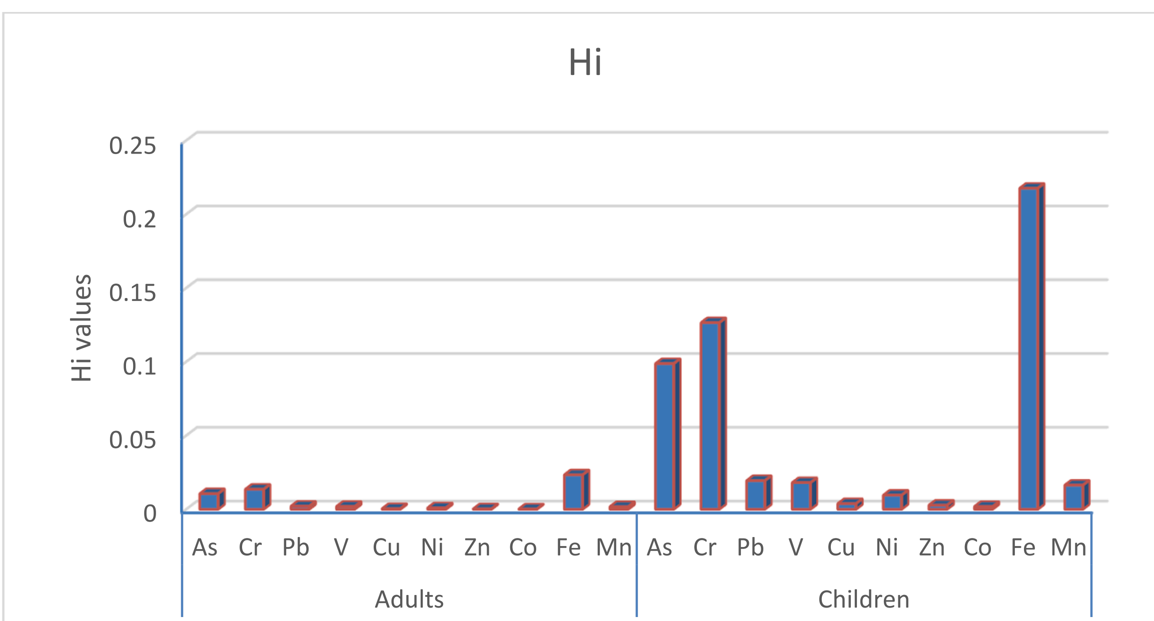

Fig. 3. The HI for non-carcinogenic risk in adults and children.

(one sample), and Gysiorthids and Calciorthids (one sample) as illustrated in Fig. 2. A significant 93.33 % of soil samples from the study area were identified as Haplaquepts and Eutrochrepts (Sheta, 2004). Haplaquepts and Eutrochrepts, classified as Inceptisols, exhibit only minimal alteration of the parent material due to soil-forming processes. These soils are found and cultivated in the eastern province of Saudi Arabia, particularly in low-lying areas with abundant natural springs. Haplaquepts, specifically, are poorly drained Inceptisols originating in deep, loamy deposits in the lower landscape regions, with the water table either at or near the surface unless drainage is implemented. Their texture primarily ranges from sandy loam to loam, and they vary in salinity from slightly saline to strongly saline.

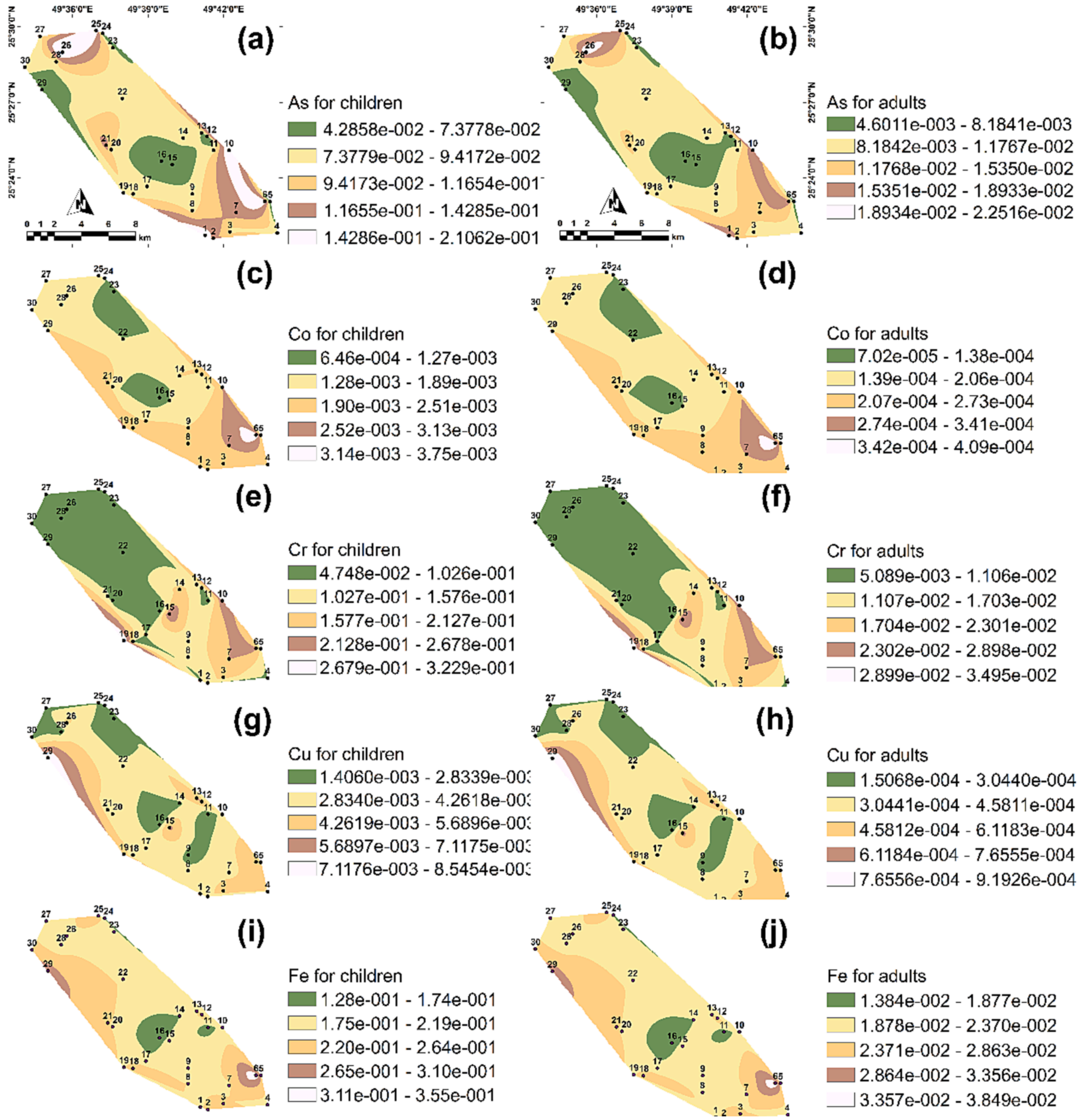

Fig. 4. Spatial distribution of hazard index (HI) of As, Co, Cr, Cu, and Fe per sampled location.

Eutrochrepts belong to the Inceptisols category and exhibit better drainage compared to Haplaquepts. These soils form in deep, loamy deposits and can vary in salinity from slightly to strongly saline. Gysiorthids and Calciorthids fall under the Aridisols classification, characterized by dry conditions with limited available moisture. Gysiorthids feature a gypsic or petrogypsic horizon within 1 m of the soil surface. They have a loamy or loamy skeletal texture, predominantly sandy loam, fine sandy loam, or loam, with corresponding gravely and very gravely variations. Calciorthids, also Aridisols, accumulate secondary carbonates to create a calcic horizon. They range from shallow to deep and have a sandy to loamy texture. Torripsamments are Entisols, forming on well-sorted sandy deposits in stream terraces, are categorized as having a torrid moisture regime and are mostly nonsaline.

The concentration of PTEs in the study area is shown in Table 1. Table 2 shows the average values of PTEs in the study area and compares them to those found in the sediment quality recommendations, the earth's crust, and some Saudi soil. The descending order of PTEs averages (dry weight, micrograms per gram) was Fe (11790) > Mn (176.43) > Zn (54.43) > Cr (28.67) > Ni (14.53) > V (12.33) > Cu (10.83) > Pb (5.23) > Co (2.87) > As (2.27). The highest levels of PTEs were recorded in S6 (Co, Fe, Mn, Ni, Pb, and V), S15 (Zn), S19 (Cr), S26 (As), and S29 (Cu). Our average values of Ni, Zn, Pb, Cr, V were less than those reported in Table 2 for several continental earth crust and Saudi Arabian soils (Yaroshevsky, 2006; Rudnick and Gao, 2003; Turekian and Wedepohl, 1961; Taylor, 1964; Al-Boghdady and Hassanein, 2019; Alharbi and El-Sorogy, 2021).

3.2. *Health risk assessment*

Many PTEs are known to be nutritionally essential and are required in minimal quantities. For example, chromium participates in the carbohydrate and lipid metabolism in the body, cobalt is the main

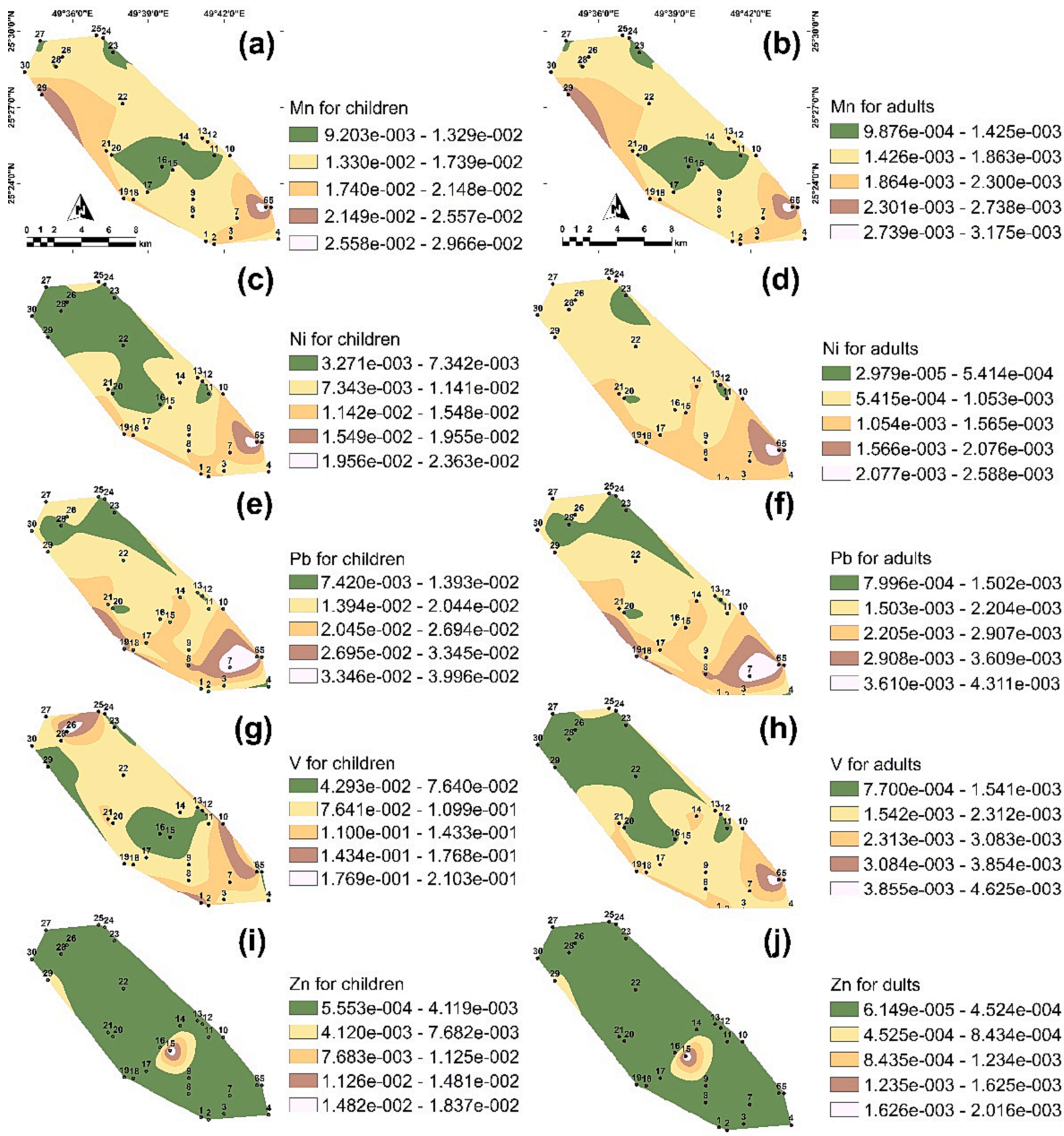

Fig. 5. Spatial distribution of hazard index (HI) of Mn, Ni, Pb, V, and Zn per sampled location.

Table 4
Average CRs and LCR for PTEs in the study area.

HMs	Adults				Children			
	CR $_{Ing.}$	CR $_{Dermal}$	CR $_{Inhal}$	LCR	CR $_{Ing.}$	CR $_{Dermal}$	CR $_{Inhal}$	LCR
As	4.658×10^{-6}	1.640×10^{-8}	6.849×10^{-11}	4.67×10^{-6}	4.347×10^{-5}	7.652×10^{-8}	3.196×10^{-10}	4.35×10^{-5}
Cr	1.963×10^{-5}	4.373×10^{-8}	2.887×10^{-10}	1.97×10^{-5}	1.833×10^{-4}	2.041×10^{-7}	1.348×10^{-9}	1.83×10^{-4}
Pb	6.094×10^{-8}	1.858×10^{-10}	8.961×10^{-13}	6.11×10^{-8}	5.687×10^{-7}	8.672×10^{-10}	4.182×10^{-12}	5.70×10^{-7}

constituent of cobalamin, manganese regulates many enzymes in the body, iron is a constituent of hemoglobin and myoglobin, nickel is required for the active synthesis of urease in plant cells, zinc is a cofactor for certain enzymes (Häder et al., 2021; Khaleeq et al., 2022). Overexposure to them can be hazardous and can cause a number of serious illnesses. For instance, an excessive amount of iron can cause a number of grave health issues, including diabetes, cancer, heart disease, and neurological abnormalities (Abbaspour et al., 2014, Al-kahtany et al., 2023b). Exposure to nickel in the workplace results in ailments such as kidney disorders, cardiovascular diseases, lung fibrosis and respiratory tract cancer. Excessive levels of manganese lead to ailments of the nervous system (Neal and Guilarte, 2013; Nour et al., 2022). Comparably,

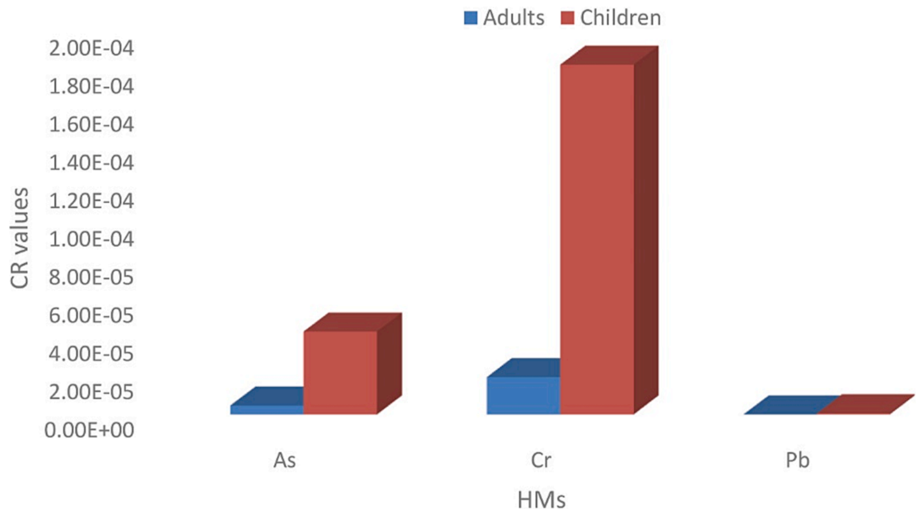

Fig. 6. Carcinogenic risks (CRs) for or As, Cr, and Pb, in adults and children.

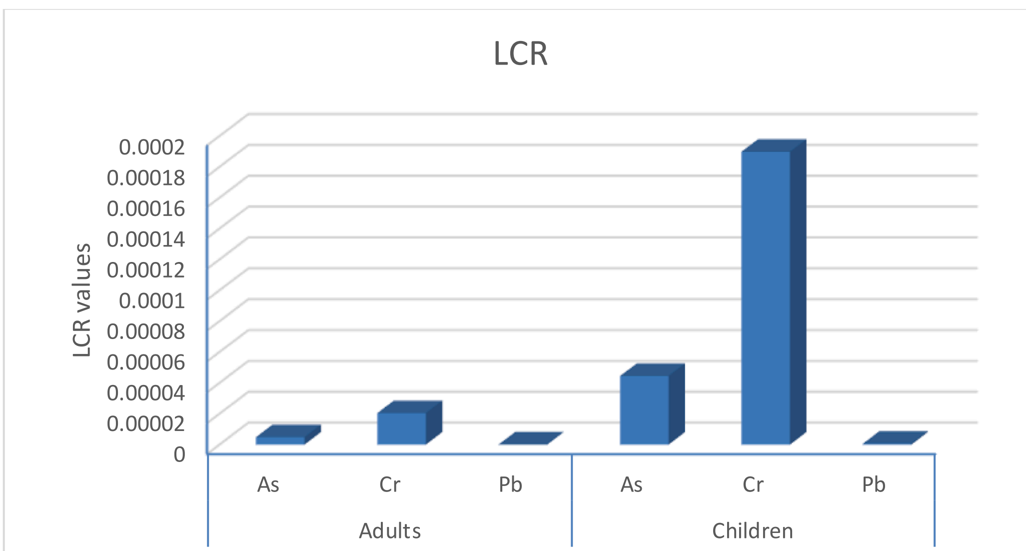

Fig. 7. The total carcinogenic risk (LCR) for or As, Cr, and Pb, in adults and children.

occupational exposure to chromium (VI) compounds in the chromate industry can result in lung cancer, irritated and ulcerated skin, burns in sensitive workers, and asthma and other respiratory distresses (Wilbur et al., 2012).

3.2.1. Chronic daily intake (CDI) and hazard index (HI)

Table 3 presents the average values of the CDI, HQ and HI for non-carcinogenic risk of PTEs from ingestion, inhalation, and dermal contact pathways on adults and children. The CDI values for adults and children took the order of CDI $_{Ing.}$ > CDI $_{Der.}$ > CDI $_{Inh.}$ The maximum CDI values (mg/kg/day) for adults were 1.615×10^{-2}, 7.215×10^{-5}, and 2.375×10^{-7} through the ingestion, dermal and inhalation pathways, respectively, while in children, the maximum CDI were 1.507×10^{-1}, 3.367×10^{-4}, and 1.108×10^{-6}, respectively. In contrast, the average CDI (mg/kg/day) from ingestion pathway in children for all PTEs shows a rise approximated nine times compared to adults, suggesting that children were at higher risk of non-carcinogenic exposure than adults. The higher CDI due to ingestion of soil by the children may be attributed to the sensitivity of children to the exposure and absorb toxic PTEs during their outdoor play activities in sediments than adults (Gevorgyan et al., 2017). However, the children's computed hazard quotient (HQ) appears to be higher than the adult's HQ (Table 3).

The HI values varied from 1.969×10^{-4} to 2.318×10^{-2} for Adults, and from 1.835×10^{-3} to 2.158×10^{-1} for children (Table S1). The hazard index for PTEs was higher among children for 9 to 9.5 times than adults. The results demonstrated that the most likely way for individuals to be exposed to PTEs in the study area was by ingestion (Chonokhuu et al., 2019). The contribution of HQing to HI for adults and children accounted 99.60 % and 99.80 % of the total risk, respectively. The HI values showed the following descending order for both adults and children: Fe > Cr > As > Pb > V > Mn > Ni > Cu > Zn > Co (Table 3, Fig. 3). The PTEs in the study area had HI values less than 1.0, indicating that residents of Al-Ahsa Oasis are not at significantly non-carcinogenic risk (Bello et al., 2019; Tian et al., 2020; Ahmad et al., 2021). However, the value of HI for Fe was greater than 0.2 for children, indicating the need to protect their health. Children are more vulnerable to the health impacts and appear to be highly susceptible to PTEs due to oral and finger practice (Agyeman et al., 2021a, b).

The spatial distribution of the HI of the PTEs per sample location for both children and adults showed similar color patterns and hotspots in S1, S2, S6, and S7 in southeastern part of the study area, and S10, S25, and S26 in the northwestern part (Figs. 4 and 5). S7 collected from palm

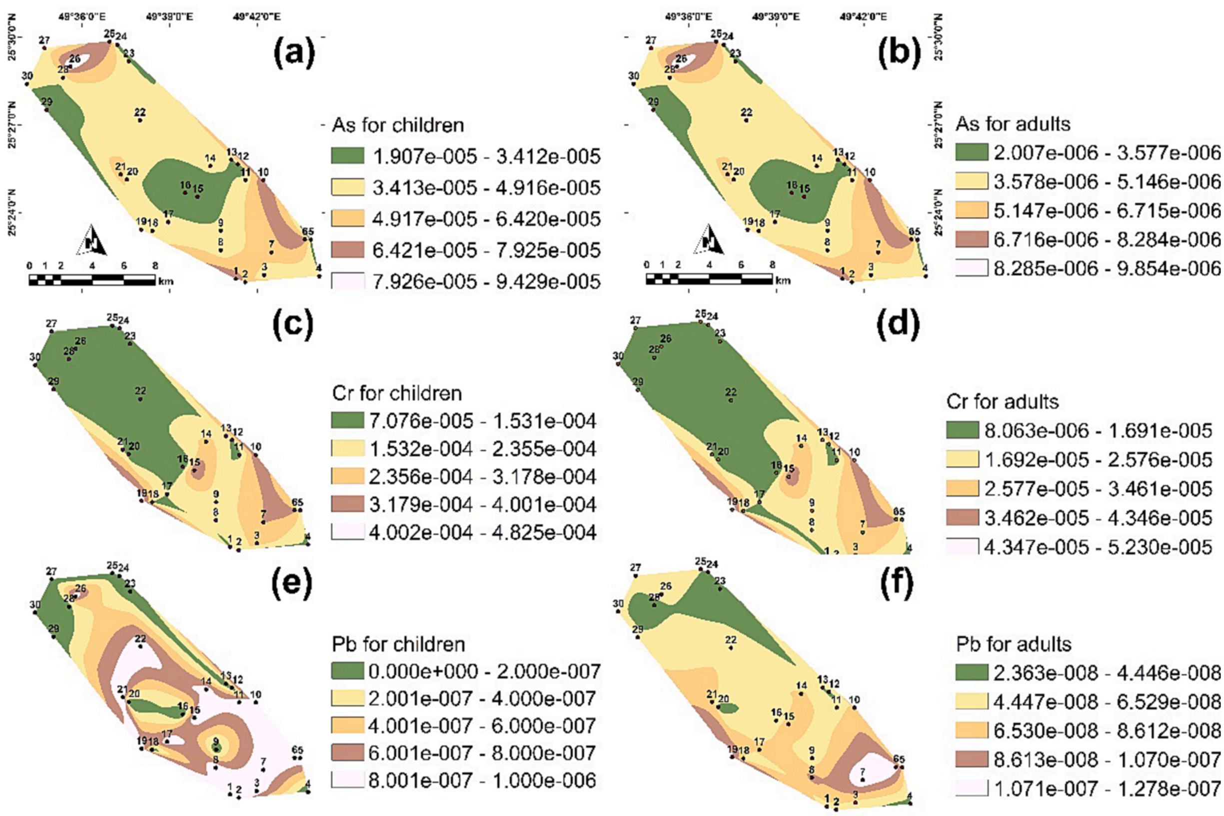

Fig. 8. Spatial distribution of LCR for As, Cr, and Pb per sampled location.

fields irrigated with treated sewage water, while S1, S2, S6, S10, S25, and S26 were irrigated with groundwater. Alharbi and El-Sorogy (2023) indicated that the Al-Ahsa soils were moderately severe enriched with As and minor to negligibly enriched with the remaining PTEs.

3.2.2. Carcinogenic risks (CRs) and total lifetime cancer risk (LCR)

Hazardous consequences may arise from an excessive build-up of toxic PTEs in human bodies. Several investigations have demonstrated that the accumulation of PTEs negatively affects immune system, central nervous system, endocrine, cardiovascular, and urogenital systems, as well as normal cellular metabolism (Wang, 2013; Wang et al., 2015; Agyeman et al., 2021). PTEs cause various health issues in children, including poor respiratory function, cardiovascular disease, reproductive toxicity, cognitive deficits, and bone damage (Madrigal et al., 2018). The CRs for Cr, As, and Pb in children was found to be significantly greater than that of adults (Table 4, Fig. 6). Average CR values in ingestion, dermal, and inhalation pathways of the adults varied from 6.094×10^{-8} to 1.963×10^{-5}, from 1.858×10^{-10} to 4.373×10^{-8}, and from 8.961×10^{-13} to 2.887×10^{-10}, respectively, while in children the CRs varied from 5.687×10^{-7} to 1.833×10^{-4}, from 8.672×10^{-10} to 2.041×10^{-7}, and from 4.182×10^{-12} to 1.348×10^{-9}, respectively. Children's CR values for Cr, As, and Pb are higher than those for adults, suggesting that children are still more likely to be exposed to PTEs due to their behavioral habits that enhance their tendency for skin contact, especially with hands (Agyeman et al., 2021; Alzahrani et al., 2023).

LCR values for Cr, As, and Pb in all studied sites were higher in children than that of the adult (Table S2). LCR values varied between adults and children from 1.97×10^{-5} to 1.83×10^{-4} (Cr), from 4.67×10^{-6} to 4.35×10^{-5} (As), and from 6.11×10^{-8} to 5.70×10^{-7} for Pb, respectively (Table 4, Fig. 7). Carcinogenic risk of the ingestion pathway was the principal contributor to the total lifetime cancer risk. It reached 99.70 % for the three PTEs in adults, while in children it reached 99.93 % for As, 99.78 % for Pb, and approximated 100 % for Cr. The spatial distribution of the LCR for the As, Cr, and Pb per sample location suggested similar color patterns for both children and adults with increase values in children (Fig. 8). LCR values of Cr in 25 samples (83.30 %) reported values slightly greater than 1×10^{-4} for children, indicating the risk is unacceptable compared to the other two HMs, which were between 1×10^{-4} and 1×10^{-6}, and lower than 1×10^{-6}, indicating acceptable or tolerable carcinogenic risk and no significant health hazards, respectively (Mondal et al., 2021; Al-Kahtany and El-Sorogy, 2023; Ahmad et al., 2023a, b).

4. Conclusions

The health risks associated with Fe, Mn, Zn, Cr, Ni, V, Cu, Pb, Co, and As in soil collected from palm farms in Al-Ahsa oasis were highlighted in this study. For every PTE, children's CDI and HI values were higher than those of adults. HI values were less than 1.0, suggesting there is no significant non-carcinogenic risk to the people inhabiting the Al-Ahsa Oasis. Moreover, the CRs and LCR for Cr, As, and Pb in children were significantly greater than those of adults, indicating that children are more susceptible than adults to health concerns associated with PTEs. LCR values for As, Cr, and Pb ranged from no significant, acceptable to tolerable carcinogenic risk health hazards, with few higher values for Cr in children. This study could be used to track any improvements or additional deterioration over time by establishing baseline PTE hazards related to Al-Ahsa oasis.

Author contributions

[TA] and [ASE] collecting samples, preparing samples for chemical analysis; [TA], [ASE], and [KA] writing manuscript and interpreting chemical analysis. All authors read and approved the final manuscript.

Declaration of competing interest

The authors declare that they have no known competing financial interests or personal relationships that could have appeared to influence the work reported in this paper.

Acknowledgments

The authors extend their appreciation to Researchers Supporting Project number (RSPD2024R791), King Saud University, Riyadh, Saudi Arabia.

Appendix A. Supplementary material

Supplementary data to this article can be found online at https://doi.org/10.1016/j.arabjc.2023.105592.

References

Abbaspour, N., Hurrell, R., Kelishadi, R., 2014. Review on iron and its importance for human health. J. Res. Med. Sci. 19 (2), 164–174.
Agyeman, P.C., Ahado, S.K., John, K., et al., 2021a. Health risk assessment and the application of CF-PMF: a pollution assessment-based receptor model in an urban soil. J. Soils Sediments 1–20. https:// doi. org/ 10. 1007/s11368- 021- 02988-x.
Agyeman, P.C., John, K., Kebonye, N.M., Borůvka, L., Vašat, R., Drabek, O., Němeček, K., 2021b. Human health risk exposure and ecological risk assessment of potentially toxic element pollution in agricultural soils in the district of Frydek Mistek, Czech Republic: a sample location approach. Environ. Sci. Eur. 33, 137. https://doi.org/10.1186/s12302-021-00577-w.
Ahmad, W., Alharthy, R.D., Zubair, M., et al., 2021. Toxic and heavy metals contamination assessment in soil and water to evaluate human health risk. Sci. Rep. 11, 17006. https://doi.org/10.1038/s41598-021-94616-4.
Ahmad, W., Zubair, M., Ahmed, M. et al. 2023a. Assessment of potentially toxic metal (loid)s contamination in soil near the industrial landfill and impact on human health: an evaluation of risk. Environ Geochem Health 45, 4353–4369 (2023). https://doi.org/10.1007/s10653-023-01499-7.
Ahmed, M., Shafqat, S.S., Javed, A., Sanaullah, M., Shakoor, A., Shafiq, M.I., Shahzadi, S. K., Wani, T.A., Zargar, S., 2023b. Exposure Assessment of essential and potentially toxic metals in wheat-based sweets for human consumption: Multivariate analysis and risk evaluation studies. Molecules 28, 7365. https://doi.org/10.3390/molecules28217365.
Al Tokhais, A.S., Rausch, R., 2008. The hydrogeology of Al Hassa Springs. In Proceedings of the 3rd International Conference on Water Resources and Arid Environments and the 1st Arab Water Forum, Riyadh, Saudi Arabia, 16–19 November 2008.
Alarifi, S.S., El-Sorogy, A.S., Al-kahtany, K., Alotaibi, M., 2022. Contamination and environmental risk assessment of potentially toxic elements in soils of palm farms in Northwest Riyadh, Saudi Arabia. Sustainability 14, 15402.
Alarifi, S.S., El-Sorogy, A.S., Al-kahtany, K.h., Hazaea, S.A., 2023. Contamination and health risk assessment of potentially toxic elements in Al-Ammariah agricultural soil, Saudi Arabia. J. King Saud Univ. – Sci. 35, 102826.
Al-Boghdady, A.A., Hassanein, K.M.A., 2019. Chemical analysis and environmental impact of heavy metals in soil of wadi Jazan area, southwest of Saudi Arabia. Appl. Ecol. Environ. Res. 17, 7067–7084.
Al-Dosary, N.M.N., 2022. Evaluation of soil characteristics for agricultural machinery management and cropping requirements in ALAflaj Oasis. Saudi Arabia. Sustainability 14, 7991.
Alharbi, T., Abdelrahman, K., El-Sorogy, A.S., Ibrahim, E., 2023. Contamination and health risk assessment of groundwater along the Red Sea coast, Northwest Saudi Arabia. Mar. Pollut. Bull. 192, 115080 https://doi.org/10.1016/j.marpolbul.2023.115080.
Alharbi, T., El-Sorogy, A.S., 2021. Spatial distribution and risk assessment of heavy metals pollution in soils of marine origin in central Saudi Arabia. Mar. Pollut. Bull. 170, 112605.
Alharbi, T., El-Sorogy, A.S., 2023. Risk assessment of potentially toxic elements in agricultural soils of Al-Ahsa Oasis, Saudi Arabia. Sustainability 15, 659. https://doi.org/10.3390/su15010659.
Alharbi, T., Nour, H., Al–Kahtany, Kh. Giacobbe, S., El–Sorogy, A. S., 2023. Sediment's quality and health risk assessment of heavy metals in the Al–Khafji area of the Arabian Gulf, Saudi Arabia. Environmental Earth Sciences 82, 471. https://doi.org/10.1007/s12665-023-11171-z.
Al-Hashim, M.H., El-Sorogy, A.S., Alshehri, F., Qaisi, S., 2022. Environmental assessment of surface seawater in Al-Uqair Coastline, Eastern Saudi Arabia. Water 14, 3423.
Al-Kahtany, K.h., El-Sorogy, A.S., 2023. Contamination and health risk assessment of surface sediments along Ras Abu Ali Island, Saudi Arabia. J. King Saud Univ. – Sci. 35, 102509 https://doi.org/10.1016/j.jksus.2022.102509.
Al-Kahtany, K.h., Nour, H.E., El-Sorogy, A.S., Alharbi, T., 2023. Ecological and health risk assessment of heavy metals contamination in mangrove sediments, Red Sea Coast. Mar. Pollut. Bull. 192, 115000 https://doi.org/10.1016/j.marpolbul.2023.115000.
Al-Kahtany, K.h., Nour, H.E., Giacobbe, S., Alharbi, T., El-Sorogy, A.S., 2023. Heavy metal pollution in surface sediments and human health assessment in southern Al-Khobar coast, Saudi Arabia. Mar. Pollut. Bull. 187, 114508 https://doi.org/10.1016/j.marpolbul.2022.114508.
Alzahrani, H., El-Sorogy, A.S., Qaysi, S., Alshehri, F., 2023. Contamination and risk assessment of potentially toxic elements in Coastal Sediments of the Area between Al-Jubail and Al-Khafji, Arabian Gulf, Saudi Arabia. Water 15, 573. https://doi.org/10.3390/w15030573.
Assubaie, F.N., 2015. Assessment of the levels of some heavy metals in water in Alahsa Oasis farms, Saudi Arabia, with analysis by atomic absorption spectrophotometry. Arab. J. Chem. 8, 240–245.
Bello, S., Nasiru, R., Garbab, N.N., Adeyemo, D.J., 2019. Carcinogenic and non-carcinogenic health risk assessment of heavy metals exposure from Shanono and Bagwai artisanal gold mines, Kano state, Nigeria. Sci. Afr. 6, e00197.
Chonokhuu, S., Batbold, C., Chuluunpurev, B., Battsengel, E., Dorjsuren, B., Byambaa, B., 2019. Contamination and health risk assessment of heavy metals in the soil of major cities in Mongolia. Int. J. Environ. Res. Public Health 16, 2552. https://doi.org/10.3390/ijerph16142552.
Chowdhury, S.h., Al-Zahrani, M., 2015. Characterizing water resources and trends of sector wise water consumptions in Saudi Arabia. J. King Saud Univ. – Eng. Sci. 27, 68–82.
Dissanayake, C.B., Chandrajith, R., 2009. Introduction to medical geology, focus on tropical environments. Springer-Verlag, Berlin Heidelberg, p. 297.
El-Kady, A.A., Abdel-Wahhab, M.A., 2018. Occurrence of trace metals in foodstuffs and their health impact. Trends Food Sci Technol 75, 36–45.
El-Sorogy, A., Youssef, M., Al-Kahtany, K.h., 2016. Integrated assessment of the Tarut Island coast, Arabian Gulf, Saudi Arabia. Environ. Earth Sci. 75, 1336.
El-Sorogy, A.S., Youssef, M., Al-Kahtany, K.h., 2021. Evaluation of coastal sediments for heavy metal contamination, Yanbu area, Red Sea coast, Saudi Arabia. Mar. Pollut. Bull. 163, 111966.
El-Sorogy, A.S., Youssef, M., Al-Hashim, M.H., 2023. Water quality assessment and environmental impact of heavy metals in the Red Sea Coastal Seawater of Yanbu, Saudi Arabia. Water 15, 201. https://doi.org/10.3390/w15010201.
Gevorgyan, G.A., Ghazaryan, K.A., Movsesyan, H.S., Zhamharyan, H.G., 2017. Human health risk assessment of heavy metal pollution in soils around kapan mining area, Armenia. Electron. J. Nat. Sci. 2 (29), 29–33.
Häder, D-P, Helbling, E.W., Villafañe, V.E, 2021. Anthropogenic Pollution of Aquatic Ecosystems. Springer Nature Switzerland. 426 p. https://doi.org/10.1007/978-3-030-75602-4.
Hashem, M.A., Nur-A-Tomal, M.S., Mondal, N.R., Rahman, M.A., 2017. Hair burning and liming in tanneries is a source of pollution by arsenic, lead, zinc, manganese and iron. Environ. Chem. Lett. 15 (3), 501–506.
IARC., 2012. A review of human carcinogens: Personal habits and indoor combustions; World Health Organization: Lyon, France, Volume 100.
Ilyas, M., Ahmad, W., Khan, H., Yousaf, S., Yasir, M., Khan, A., 2019. Environmental and health impacts of industrial wastewater effluents in Pakistan: a review. Rev. Environ. Health 34 (2), 171–186. https://doi.org/10.1515/reveh-2018-0078.
IRIS. Program Database., 2020. Available online: https://cfpub.epa.gov/ncea/iris/search/index.cfm (accessed on 18 September 2020).
Jaishankar, M., Tseten, T., Anbalagan, N., Mathew, B.B., Beeregowda, K.N., 2014. Toxicity, mechanism and health effects of some heavy metals. Interdisc. Toxicol. 7 (2), 60–72.
Kabata-Pendias, A., 2011. Trace Elements of Soils and Plants, 4th ed.; CRC Press: Boca Raton, FL, USA; Taylor & Francis Group, LLC: Abingdon, UK, p. 505.
Kahal, A.Y., El-Sorogy, A.S., Qaysi, S.I., Al-Hashim, M.H., Al-Dossari, A., 2023. Environmental Risk Assessment and Sources of Potentially Toxic Elements in Seawater of Jazan Coastal Area, Saudi Arabia. Water 15, 3174.https://doi.org/10.3390/w15183174.
Khaleeq, A., Ahmed, M., Huma, R., Mujtaba, A., Noor, S., Rehman, R., Sheikh, T.A., Qamar, S., et al., 2022. Evaluation of trace and heavy metals in different varieties of sauces to characterize their impact on human health. J. Food Compos. Anal. 114, 104789 https://doi.org/10.1016/j.jfca.2022.104789.
Luo, X.S., Ding, J., Xu, B., Wang, Y.J., Li, H.B., Yu, S., 2012. Incorporating bioaccessibility into human health risk assessments of heavy metals in urban park soils. Sci. Total Environ. 424, 88–96.
Madrigal, J., Persky, V., Pappalardo, A., Argos, M., 2018. Association of heavy metals with measures of pulmonary function in youth: findings from the 2011–2012 National Health and Nutrition Examination Survey (NHANES). ISEE Conf. Abstr. 2018. https:// doi. org/ 10. 1289/ isesi see. 2018.03. 03. 26.
Ministry of Environment, Water and Agriculture (MEWA), 1986. General Soil Map of the Kingdom of Saudi Arabia (Soil Atlas); Department of Lands Investment Management (Formerly): Riyadh, Saudi Arabia (In Arabic).
Mishra, S., Bharagava, R.N., More, N., Yadav, A., Zainith, S., Mani, S., Chowdhary, P., 2019. Heavy metal contamination: an alarming threat to environment and human health. In: Sobti, R.C., Arora, N.K., Kothari, R. (Eds.), Environmental Biotechnology: for Sustainable Future. Springer, Singapore, pp. 103–125. https://doi.org/10.1007/978-981-10-7284-0_5.
Mondal, P., Lofrano, G., Carotenuto, M., Guida, M., Trifuoggi, M., Libralato, G., Sarkar, S. K., 2021. Health risk and geochemical assessment of trace elements in surface sediment along the Hooghly (Ganges) River Estuary (India). Water 13, 110.
Neal, A.P., Guilarte, T.R., 2013. Mechanisms of lead and manganese neurotoxicity. Toxicol. Res. (Camb.) 2 (2), 99–114. https://doi.org/10.1039/c2tx20064c.
Nour, H.N., Alshehri, F., Sahour, H., El-Sorogy, A.S., Tawfik, M., 2022. Assessment of heavy metal contamination and health risk in the coastal sediments of Suez Bay, Gulf of Suez, Egypt. J. Afr. Earth Sci. 195, 104663 https://doi.org/10.1016/j.jafrearsci.2022.104663.

Praveena, S.M., Pradhan, B., Ismail, S.N.S., 2015. Spatial assessment of heavy metals in surface soil from Klang District (Malaysia): An example from a tropical environment. Hum. Ecol. Risk Assess. 21 (7), 1980–2003. https://doi.org/10.1080/10807039.2015.1017872.

Rahman, M.S., Kumar, P., Ullah, M., Jolly, Y.N., Akhter, S., Kabir, J., Begum, B.A., Salam, A., 2021. Elemental analysis in surface soil and dust of roadside academic institutions in Dhaka city, Bangladesh and their impact on human health. Environ. Chem. Ecotoxicol. 3, 197–208.

Rudnick, R.L., Gao, S., 2003. Composition of the continental crust. The Crust 3, 1–64.

Shadfan, H., Mashhady, A., Eter, A., Hussen, A.A., 1987. Mineral composition of selected soils in Saudi Arabia. J. Soil Nutr. Soil Sci. 147, 649–802.

Sheta, A.S., 2004. Soil quality: Standards of soil quality under the conditions of Saudi Arabia, 7th ed.; Saudi Society for Agricultural Sciences, King Saud University: Riyadh, Saudi Arabia (In Arabic).

Taylor, S.R., 1964. Abundance of chemical elements in the continental crust: a new table. Geochim. Cosmochim. Acta 28, 1273–1285.

Tian, S., Wang, S., Bai, X., Zhou, D., Luo, G., Yang, Y., Hu, Z., Li, C., Deng, Y., Lu, Q., 2020. Ecological security and health risk assessment of soil heavy metals on a village-level scale, based on different land use types. Environ. Geochem. Health 42, 3393–3413. https://doi.org/10.1007/s10653-020-00583-6.

Turekian, K.K., Wedepohl, K.H., 1961. Distribution of the elements in some major units of the Earth's Crust. Geol. Soc. Amer. Bull. 72, 175–192.

US EPA, United States Environmental Protection Agency 1989. Risk assessment guidance for superfund, Vol. 1: Human health evaluation manual; Office of Soild Iste and Emergency Response: Washington, DC, USA.

USEPA, 2001. Risk Assessment Guidance for Superfund, Vol.: Volume III. Part A, Process for Conducting Probabilistic Risk Assessment; US Environmental Protection Agency: Washington, DC, USA.

USEPA, 2002. Supplemental guidance for developing soil screening levels for superfund sites. U. S. Environmental Protection Agency, Office of Emergency and Remedial Response, Washington.

Wang, Q., Liu, J., Cheng, S., 2015. Heavy metals in apple orchard soils and fruits and their health risks in Liaodong Peninsula, Northeast China. Environ. Monit. Assess. 187. https:// doi. org/ 10. 1007/ s10661- 014- 4178-7.

Wang, W.X., 2013. Dietary toxicity of metals in aquatic animals: recent studies and perspectives. Chinese. Sci. Bull. 58, 203–213. https:// doi. org/10. 1007/ s11434-012- 5413-7.

Wilbur, S., Abadin, H., Fay, M., Yu, D., Tencza, B., Ingerman, L., Klotzbach, J., James, S., 2012. Agency for toxic substances and disease registry (ATSDR) toxicological profiles. In: Toxicological profile for chromium. Agency for Toxic Substances and Disease Registry (US), Atlanta, GA.

Yaroshevsky, A.A., 2006. Abundances of chemical elements in the Earth's crust. Geoch. Internat. 44 (1), 48–55.

Zhang, J., Li, H., Zhou, Y. et al., 2018. Bioavailability and soil-to-crop transfer of heavy metals in farmland soils: a case study in the Pearl River Delta, South China. Environ. Pollut. 235, 710–719. https:// doi. org/ 10. 1016/j.envpol. 2017. 12. 106.